Sustainability assessment of concrete structure durability under reinforcement corrosion

Thybo, Anna Emilie Anusha; Michel, Alexander; Stang, Henrik

Publication date:
2013

S2-3-4

SUSTAINABILITY ASSESSMENT OF CONCRETE STRUCTURE DURABILITY UNDER REINFORCEMENT CORROSION
ICCS13 CONFERENCE PROCEEDINGS

Anna Emilie A. THYBO
PhD Student, Dept. of Civil Engineering, Technical University of Denmark, Denmark

Alexander MICHEL
Post Doc., Dept. of Civil Engineering, Technical University of Denmark, Denmark

Henrik STANG
Professor, Dept. of Civil Engineering, Technical University of Denmark, Denmark

ABSTRACT:
In the present paper a parametric study is conducted based on an existing finite element based model. The influence of cover layer, reinforcement diameter and water-to-cement ratio is compared to a possible scatter in the results due to insufficient knowledge about the distribution of the corrosion current density along the circumference of the reinforcement. Simulations show that the scatter has a greater influence on the results than changing the parameters wherefore it is concluded that further investigation of the non-uniform deposition of corrosion products is essential to better understand and predict the durability of a given structure.

Keywords: Non-uniform corrosion, reinforced concrete, concrete cover cracking, numerical modeling, parameter study, finite element method.

1. INTRODUCTION

Infrastructure construction is important in society and therefore a tremendous amount of money is spent on new construction and the maintenance of older ones. In addition to this lots of resources are used on research and development to improve the understanding of the durability of structures and thereby improve the sustainability.
One main factor to improve the sustainability is to better understand and describe the service life and associated deterioration mechanisms of a given structure. A major part of the infrastructures are made of reinforced concrete and one of the most important deterioration mechanisms in reinforced concrete structures is reinforcement corrosion [1]. Reinforcement corrosion induces deterioration mechanisms such as concrete cracking and cross sectional reduction of the reinforcement both decreasing the load bearing capacity and thereby affecting the serviceability of a structure. Based on this, especially corrosion-induced cover cracking has been studied, see e.g. [2,3], and various models such as analytical, see e.g. [4,5], empirical, see e.g. [6,7], and finite element based, see e.g. [8-11], models have been suggested over the years.
Recent experimental investigations such as x-ray attenuation [12-14] and digital image correlation [15] have shown that a) corrosion products deposit non-uniformly along the circumference of the reinforcement and b) corrosion products penetrate into the concrete matrix. Motivated by these observations an existing finite element based model [11] simulating the expansion of uniformly deposited corrosion products along the circumference of the reinforcement and predicting the propagation of corrosion-induced cracking was taken a step further implementing at first the penetration of corrosion products into the concrete matrix [15] and subsequently implementing the non-uniform formation of corrosion products in the modeling scheme [16]. The non-uniformity of the distribution of corrosion products was found to have a significant influence on the corrosion-induced fracture process.
In the present paper the updated finite element based model [16] was used to study the influence of different geometrical and material parameters on the service life. To get a better feel for the importance of the non-uniformity of corrosion products three parameters were chosen for the parametric study; a) the cover layer, b) the reinforcement diameter and c) the water-to-cement ratio. The parametric study was performed for two different distributions of the corrosion current density.

2. MODEL APPROACH

In the following a short description of the applied model is given. Further details regarding the modeling are found in [11,15,16].
An existing finite element (FE) based corrosion-induced cracking model was used to simulate the expansion of corrosion products and the subsequent crack propagation applying a discrete cracking

approach. The model simulates non-uniform corrosion in a semi-infinite defect free reinforced concrete body. Micro-cracking and the influence of cracks on transport properties of the concrete was not considered.
In the model the system is divided into five distinct domains; concrete, reinforcement, corrosion layer, cracking, and a debonding domain (crack opening and sliding at reinforcement surface). In Fig.1 the five domains are illustrated for two different times, t_1 (damage phase in service life design) and t_2 (cracking phase in service life design). As shown in Fig.1 the crack initiates at or near the surface of the reinforcement and propagates towards the concrete surface which is consistent with observations in [12-15].

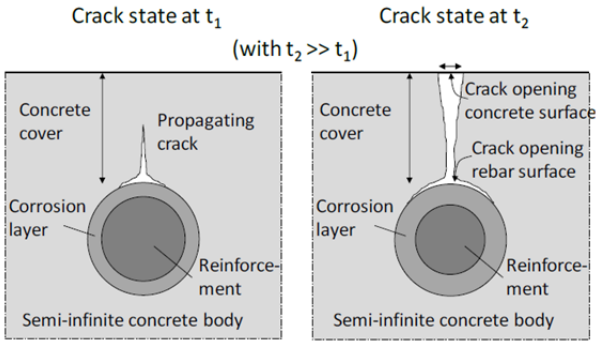

Fig.1 Crack propagation - damage (left) and cracking (right) phase - in applied FE model, from [10]

The concrete region is defined by a semi-infinite concrete body with elastic material behavior.
Based on experimental investigations [2,3] of corrosion-induced crack patterns, the zero-thickness cohesive interface elements were implemented perpendicular (simulating mode-I crack propagation in the concrete cover) and circumferential (simulating mixed-mode crack propagation) to the reinforcement allowing only for crack propagation in the implemented interface elements.

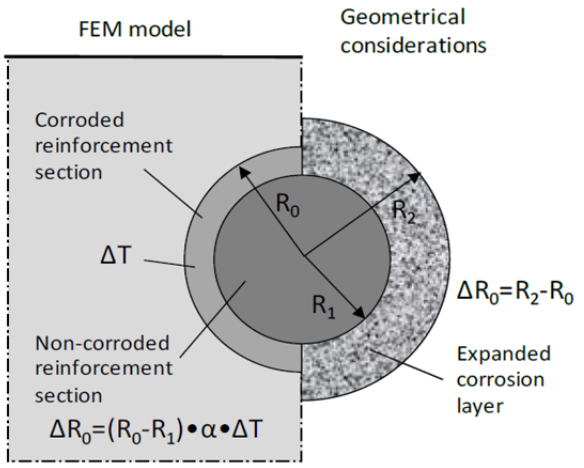

Fig.2 Load application in FE model (left) and basic geometrical considerations to model uniform formation of corrosion products (right) in the crack propagation model, from [10]

In [16] the model was taken a step further implementing non-uniform deposition of corrosion products in the modeling scheme i.e. going from the situation illustrated in Fig.2 to the situation illustrated in Fig.3. In the figures R_2 is the free expanding radius of the corroded reinforcement, R_1 the radius of the non-corroded part of the reinforcement and R_0 the radius of the original non-corroded reinforcement. In Fig.3 R_1 and R_2 vary along the circumference of the reinforcement due to the non-uniform formation of corrosion products.

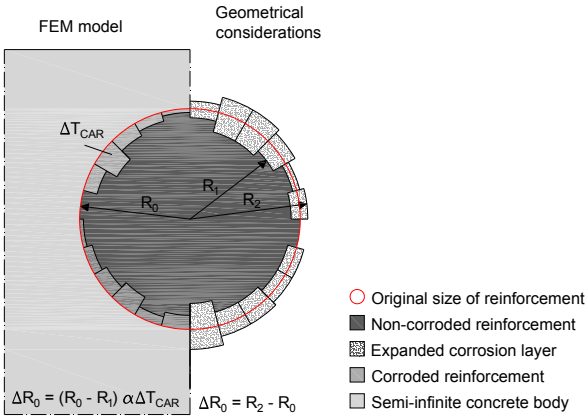

Fig.3 Load application (left) and basic geometrical considerations to model non-uniform formation of corrosion products (right) in the crack propagation model, from [16]

Due to the expansion of the corrosion products tensile stresses are developed. Cracking in the concrete cover layer is induced once the tensile stresses exceed the tensile strength of the concrete.
The expansive nature of the corrosion products was modeled determining the reduction of reinforcement area and subsequently calculating the expansion of the corrosion products.
Faraday's law was used to determine the reinforcement radius reduction due to corrosion i.e. the size of the corrosion layer. To account for the variation of R_1 and R_2, the corrosion current density along the circumference of the reinforcement was varied generating different degrees of corrosion of the reinforcement - maintaining the same total corrosion current as in the uniform case. Mathematically the non-uniformity was modeled changing the corrosion current density from a scalar to a vector. The following expression of Faraday's law was applied in the modeling:

$$\overrightarrow{X(t)} = \overrightarrow{R_0} - \overrightarrow{R_1} = (M\,\overrightarrow{i_{corr}}\,\Delta t)/(z\,F\,\rho) \qquad (1)$$

where,

M : molar mass of the metal [g/mol]
i_{corr} : corrosion current density [A/cm^2]
Δt : duration of current application [s]
z : anodic reaction valence [-]
F : Faraday's constant [A·s/mol]
ρ : density of the metal [g/cm^3]

To account for the expansion the linear expansion coefficient was introduced:

$$\eta_{lin}(\overrightarrow{R_0} - \overrightarrow{R_1}) = \overrightarrow{R_2} - \overrightarrow{R_0} \quad (2)$$

$$\eta_{lin} = \alpha \, \Delta T \quad (3)$$

where,

α : fictitious thermal expansion coefficient [K^{-1}]

ΔT : temperature increment [K]

2.1 Penetration of corrosion products into the concrete matrix

In experimental data obtained from x-ray attenuation [12-14] and digital image correlation measurements [15] it was observed that corrosion products penetrated into the concrete matrix delaying the stress formation and thereby the initiation of cracking. Therefore, based on the conceptual model in Fig.4, the mechanism was implemented in the modeling scheme in [12,15] reducing the effect of corrosion-induced expansion.

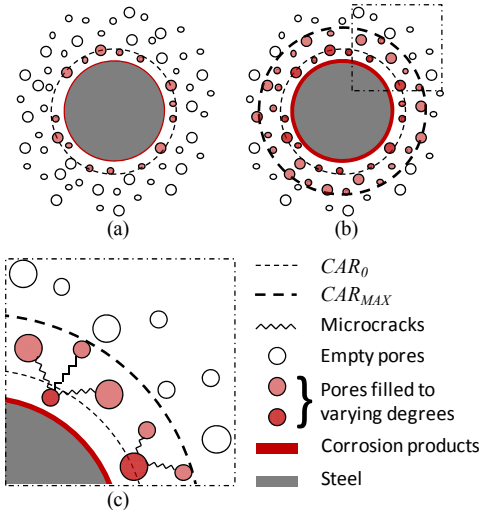

Fig.4 Conceptual schematic of idealized filling process of capillary porosity with corrosion products: (a) shows the initial *CAR*, CAR_0, (b) the subsequent increase in CAR size to a maximum, CAR_{MAX} and filling of additional pores due to (c) formation of micro-cracks between pores allowing movement of corrosion products, from [15]

In Fig.4 the penetration of corrosion products into the cementitious matrix is illustrated. Based on experimental observations, the model describes the development and expansion of a so-called corrosion accommodating region (CAR) - a region in which corrosion products penetrate the concrete matrix filling pores and moving in developed micro-cracks. A minimum (CAR_0) and a maximum (CAR_{MAX}) CAR was observed. Based on this knowledge it was possible to describe an adjusted temperature increment, see e.g. Eq. 4 and applying it in the modeling scheme instead of ΔT.

$$\overrightarrow{\Delta T_{CAR}} = \overrightarrow{\lambda_{CAR}} \, \Delta T \quad (4)$$

λ_{CAR} describes the penetration of corrosion products into the accessible space of the cementitious matrix and was determined following Eq. 5:

$$\overrightarrow{\lambda_{CAR}} = \left(\overrightarrow{V_{cp}} / \overrightarrow{V_{CAR}}\right)^n \quad if \ \overrightarrow{V_{cp}} < \overrightarrow{V_{CAR}}$$
$$\overrightarrow{\lambda_{CAR}} = \vec{1} \quad if \ \overrightarrow{V_{cp}} \geq \overrightarrow{V_{CAR}} \quad (5)$$

where,

n : empirical parameter estimated to be 1.3 in [15]

V_{cp} : volume of corrosion products

V_{CAR} : volume of CAR

The volume of the CAR is depending on the porosity and accessible volume of the concrete matrix:

$$\overrightarrow{V_{CAR}} = \varphi \ \overrightarrow{V_{CM}} \quad (6)$$

where,

φ : capillary porosity of the concrete material

V_{CM} : accessible volume of the concrete matrix depending on the size of CAR

2.2 Creep

The effect of creep was implemented in the model in [15] according to [19] where the effective modulus of elasticity of the concrete matrix is adjusted at each time step following Eq. 7.

$$E_{c,eff} = E_c / (1 + \varphi(t,t_0)) \quad (7)$$

where,

$E_{c,eff}$: effective modulus of elasticity [MPa]

E_c : tangent modulus of elasticity [MPa]

$\varphi(t,t_0)$: creep coefficient [-]

t : age of the concrete matrix [days]

t_0 : time at loading [days]

3. NUMERICAL SIMULATION

In the numerical simulation, the cover layer (C), the reinforcement diameter (D) and the water-to-cement ratio (w/c) were varied to study the influence of geometrical and material properties on two different limits states – damage limit (DL) and cracking limit (CL).

In Table 1 and Table 2, a schematic illustration of the investigated values of the cover layer, the reinforcement diameter and the water-to-cement ratio are given.

Table 1 Overview of parametric study for S90

Identification	C (mm)	D (mm)	w/c (-)
Ref_{S90}	45	10	0.4
$C25_{S90}$	25	10	0.4
$C65_{S90}$	65	10	0.4
$R5_{S90}$	45	5	0.4
$R20_{S90}$	45	20	0.4
$WC03_{S90}$	45	10	0.3
$WC05_{S90}$	45	10	0.5

Table 2 Overview of parametric study for S270

Identification	C (mm)	D (mm)	w/c (-)
Ref_{S270}	45	10	0.4
$C25_{S270}$	25	10	0.4
$C65_{S270}$	65	10	0.4
$R5_{S270}$	45	5	0.4
$R10_{S270}$	45	20	0.4
$WC03_{S270}$	45	10	0.3
$WC05_{S270}$	45	10	0.5

The damage and cracking limit were original defined in [17,18] and related to service life design as a part of the propagation phase describing corrosion-induced structural consequences in the concrete, see e.g. Fig.1 and Fig.5.

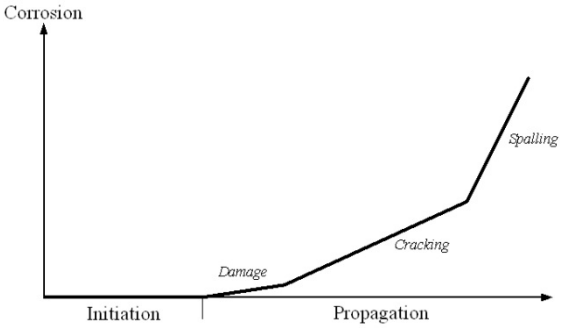

Fig.5 Model for corrosion initiation and propagation and the terminology used in the current study for characterizing the propagation phase, from [11,17,18]

Normally the end of the initiation phase - de-passivation of the reinforcement - defines the end of service life, however this limit state is difficult to find (as it is not visible) and measure, hence great uncertainty is connected to it. Thus, it was suggested in [11] to base the end of damage and cracking phase on the size of the crack width at the cover surface. Based on a literature study and experimental observations the two crack widths, 50 μm and 0.2 mm, were applied in [11] as limits for DL and CL, respectively as these crack widths are possible to both measure and observed with the naked eye. On the basis of [11] these two values were also used as limit states in this study.

Investigating the influence of non-uniform corrosion a considerable scatter was observed in [16] when considering crack width and time-to cover cracking. To investigate the influence of the scatter compared to the influence of varying C, R and w/c, the parameters were studied for two distinct situations; a) accumulation of the corrosion products at the initiation point of the predefined corrosion-induced crack path (S90) b) accumulation of the corrosion products at the opposite site of the initiation point of the predefined corrosion-induced crack path (S270). The two situations (S90 and S270) are illustrated in Fig.6 and Fig.7 showing the variation in corrosion current density along the circumference of the reinforcement. The degrees referred to in the figures are polar angle coordinates which are shown together with the location of the initiation point of the predefined corrosion-induced crack path in Fig.8.

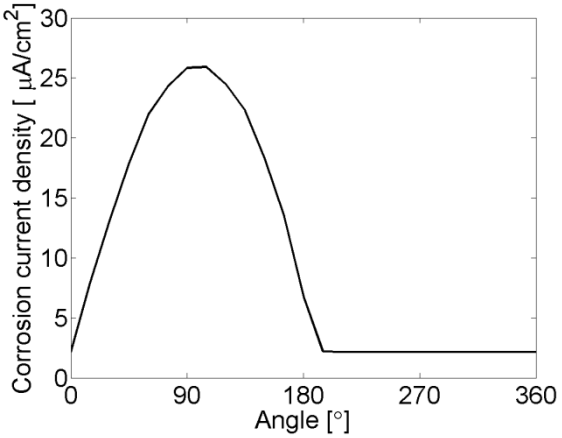

Fig.6 Variation of the corrosion current density along the circumference of the reinforcement for S90

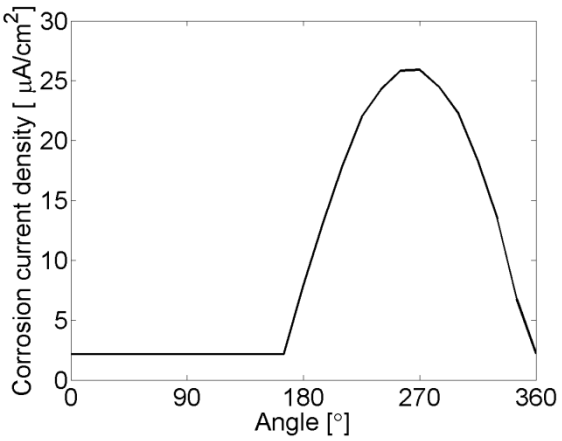

Fig.7 Variation of the corrosion current density along the circumference of the reinforcement for S270

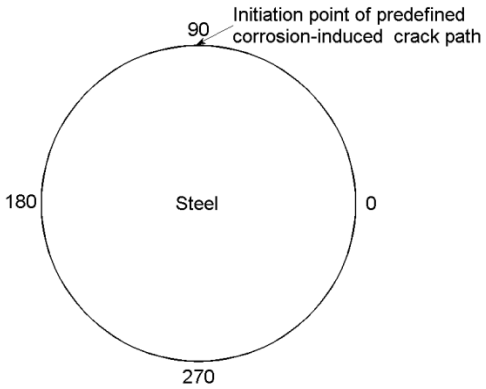

Fig.8 Polar angle coordinates held together with location of initiation point of predefined corrosion-induced crack path

In Table 3 the input parameters used in the analysis are provided. The geometrical values of the concrete were (assuming semi-infinite behavior) based on a study

presented in [10] and the linear expansion coefficient for the corrosion products was set to 0.7 assuming the formation of hematite (Fe_2O_3), which was observed by energy dispersive spectroscopy in [14]. A mean value of 10 μA/cm^2 was applied as corrosion current density as values of this size have been observed for actual structures subjected to corrosion in [17].

Table 3 Input parameters

Parameter	Value	Dimension
Length	23	mm
Width	210	mm
Height	155	mm
C	45	mm
D	10	mm
w/c	0.4	-
f_{cm}	60	MPa
f_{ctm}	4.1253	MPa
τ_c	4.1253	MPa
E_c	39.542	GPa
μ_c	0.2	-
E_s	210	GPa
μ_s	0.3	-
E_{corr}	2	GPa
μ_{corr}	0.3	-
RH	65	%
M_{Fe}	55.845	g/mol
z	2	-
ρ_{steel}	7.86	g/cm^3
F	96485	A·s/mol
$i_{corr\ mean}$	0.00001	A/cm^2
CAR_0	0.14	mm
CAR_{MAX}	0.28	mm
η_{lin}	0.7	-
α	1	-

When varying w/c material properties as compression and tensile strength as well as the modulus of elasticity of concrete were changed according to Table 4. The relation between the three parameters in Table 4 was based on guidelines given in [19,20].

Table 4 Characteristics of concrete for w/c = 0.3 and w/c = 0.5

Identification	f_{cm} (MPa)	f_{ctm} (MPa)	E_c (GPa)
WC03	85	4.7727	43.897
WC05	45	3.3311	36.272

To simulate corrosion-induced crack propagation, the commercial FEM program TNO DIANA 9.4.2 was used. 2316-2984 elements (4838-6192 nodes) were used to discretize the interface, concrete, reinforcement and corrosion layer domain in the model depending on the geometry. Nonlinear solution of the problem was obtained using a standard Newton-Raphson method with a displacement controlled convergence criterion.

4. RESULTS

Fig.9 illustrates numerical results of the time to reach the damage (DL) and cracking limit (CL) state for S90 and S270 (varying location of corrosion products see Fig.6 and Fig.7) for different cover layers. Generally it is seen that both the time to reach DL and CL depend on the size of the cover layer. Although, the effect is reverse comparing DL and CL. Increasing the cover layer increases the time to reach DL but decreases the time to reach CL i.e. the larger the cover layer the faster the crack width increases once the crack has reached the surface which corresponds well to results found in [11].

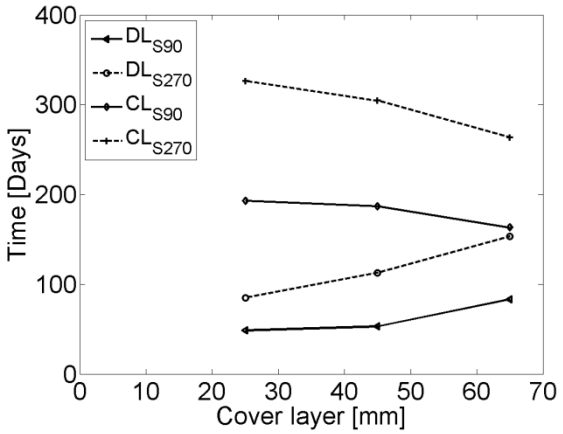

Fig.9 Time to reach damage and cracking limit comparing S90 and S270 for different cover layers

Considering the two results for DL it is seen that increasing the cover layer from 25 mm to 65 mm increases the time to reach DL with 73% and 80% for S90 and S270, respectively. Furthermore the figure shows that changing the situation from S90 to S270 increases the time to reach DL with 77% and 84% for 25 mm and 65 mm, respectively. This indicates that the time to reach DL can be the same for a 25 mm cover layer and a 65 mm cover layer depending on the corrosion conditions and thereby the distribution of the corrosion current density along the circumference of the reinforcement.

Considering the results for CL it is seen that increasing the cover layer from 25 mm to 65 mm decreases the time to reach CL with 15% and 19% for S90 and S270, respectively. This implies that the influence of size of the cover layer is more pronounced for DL than CL.

For both DL and CL one break in each curve for S90 and S270 is observed indicating that the relation between the cover layer and time to reach DL and CL is non-linear. To determine this non-linearity other values of the cover layers should also be studied. Further, the slope of the curves is steeper for S270 than S90 implying that the lower corrosion current density the more pronounced is the influence of changing the cover layer.

In Fig.10 the results of the time to reach damage and cracking limit state for different reinforcement

diameters for the two situations S90 and S270 are illustrated. Opposite to variations of the cover layer varying the reinforcement diameter affects DL and CL in the same way as all four curves descends asymptotically – the bigger the reinforcement diameter the earlier the limit state is reached indicating that for a given reinforcement diameter the influence of increasing the reinforcement diameter on DL/CL is limited. Considering the two results for DL it is seen that increasing the reinforcement diameter from 5 mm to 20 mm decreases the time to reach DL with 52% and 36% for S90 and S270, respectively. The two results for CL show that the time to reach CL is decreased with 54% and 50 % for S90 and S270, respectively. This indicates that the influence of the reinforcement diameter is less pronounced for DL for lower corrosion current densities. However, further studies of this effect should be conducted to reinforce the observations of this study.

Comparing S90 and S270 show that DL increases with 80% and 139% and CL increases with 61% and 72% for 5 mm and 20 mm indicating that generally DL is more susceptible to changes in reinforcement diameter than CL and the effect gets more pronounced for larger reinforcement diameters. It is seen, comparing the different percentages, that the influence of the distribution of the corrosion current density, in this case, is greater than the influence of the reinforcement diameter.

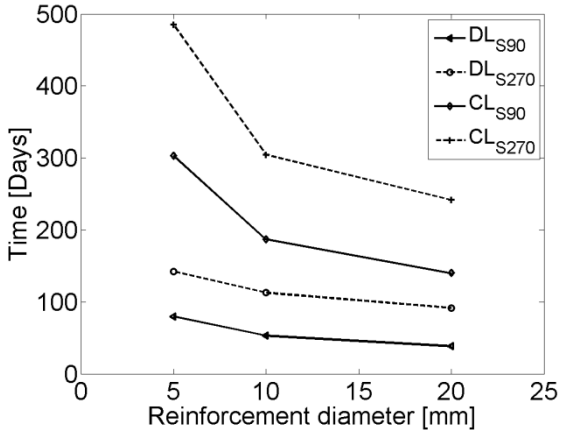

Fig.10 Time to reach damage and cracking limit comparing S90 and S270 for different reinforcement diameters

Fig.11 illustrates the modeled time to reach the damage and cracking limit states for different water-to-cement ratios. Generally it is seen that varying w/c affects the results less than varying the cover layer and the reinforcement diameter. One reason for this is most likely that w/c affects other material parameters, which may counteract each other, e.g. tensile strength and the modulus of elasticity, when considering the propagation of cracks. However, a main aspect in this paper is to compare the influence of certain parameters (i.e. water-to-cement ratio, cover layer, reinforcement diameter and distribution of corrosion current density) on DL and CL - whereby a detailed sensitivity analysis of other affected material parameters, such as tensile strength and modulus of elasticity, has not been conducted.

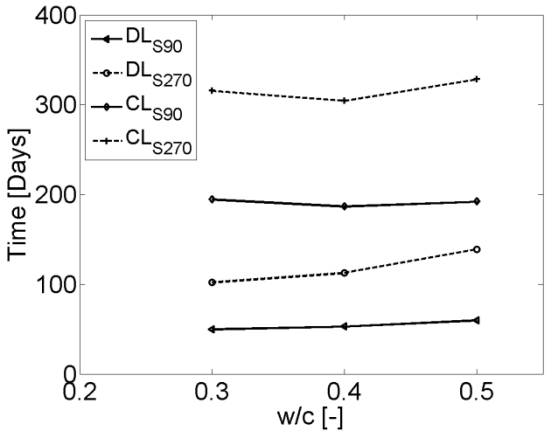

Fig.11 Time to reach damage and cracking limit comparing S90 and S270 for different w/c

Increasing the w/c from 0.3 to 0.5 increases the time to reach DL viz. 20% for S90 and 36% for S270. Considering CL; S90 decreases with 2% and S270 increases with 4% indicating that the influence of w/c on CL is insignificant. It is seen that the slope of S270 is changing from negative to positive, however this is neglected as the decrease and increase is only 3% and 8%, respectively.

Comparing S90 and S270 the time to reached both DL and CL is significantly improved for S270 as the time is raised with more than 50% in average. This clearly shows that the uncertainty of the distribution of the corrosion current density is more decisive than varying w/c.

To create an overview, the results from the parametric study are arranged in tabular form in Table 5.

Table 5 Time to reach damage and cracking limit based on Faraday's law

Identification	DL (days)	CL (days)
Ref_{S90}	52	186
Ref_{S270}	112	304
$C25_{S90}$	48	192
$C25_{S270}$	85	326
$C65_{S90}$	83	163
$C65_{S270}$	153	263
$R5_{S90}$	79	302
$R5_{S270}$	142	485
$R20\_{S90}$	38	140
$R20_{S270}$	91	241
$WC03_{S90}$	49	194
$WC03_{S270}$	102	315
$WC05_{S90}$	59	191
$WC05_{S270}$	139	328

5. SUMMARY AND CONCLUSIONS

In the present paper an existing finite element based

model simulating the expansion of non-uniformly deposited corrosion products - taking into account the penetration of corrosion products into the concrete matrix and predicting the propagation of corrosion-induced cracking was used to investigate the influence of cover layer, reinforcement diameter and water-to-cement ratio on the damage and cracking limit state. The importance of three parameters was shown together with the influence of uncertainty of the distribution of the corrosion current density varying the parameters for two different situations; a) accumulation of corrosion products at the initiation point of the predefined corrosion-induced crack path b) accumulation of corrosion products at the opposite site of the initiation point of the predefined corrosion-induced crack path. On the basis of the presented results the following was concluded:

(1) In the parametric range investigated, the uncertainty observed due to insufficient knowledge about the distribution of the corrosion current density along the circumference of the reinforcement overrules the effects of changing the studied parameters, i.e. cover layer thickness, reinforcement diameter, and water-to-cement ratio.
(2) Increasing the cover layer increases the time to reach the damage limit but decreases the time to reach the cracking limit, although the damage limit seems to be more susceptible to changes.
(3) Varying the cover layer affected the curves representing situation b) (accumulation of corrosion products at the opposite site of the initiation point of the predefined corrosion-induced crack path) the most indicating that the lower corrosion current density the more pronounced is the influence of varying the cover layer.
(4) Increasing the reinforcement diameter results in an asymptotically descending curve indicating that for a given reinforcement diameter the influence of increasing the reinforcement diameter on damage and cracking limit is limited.
(5) The influence of changing the water-to-cement ratio is limited.

Based on the conclusions the importance of investigating the distribution of the corrosion current density along the circumference of the reinforcement is visualized. As the distribution appears to be random, a probabilistic approach may be used to implement the uncertainty. Implementation of such a probabilistic modeling approach in the modeling scheme would give a more realistic estimate of the durability of a given structure and thereby improve the sustainability of the structure.

ACKNOWLEDGEMENT

The authors gratefully acknowledge the financial support of the Danish Expert Centre for Infrastructure Constructions.

REFERENCES

1. Rendell, F., Jauberthie, R. and Grantham, M., "Deteriorated Concrete - Inspection and physicochemical analysis," Thomas Telford, 2002.
2. Alonso, C., Andrade, C., Rodriguez, J. and Diez, J., "Factors controlling cracking of concrete affected by reinforcement corrosion," Materials and Structures, 1998, Vol.31, pp. 435-441.
3. Andrade, C., Alonso, C. and Molina, F. J., "Cover cracking as a function of bar corrosion: Part 1-Experimental test," Materials and Structures, 1993, Vol.26, pp. 453-464.
4. Liu, Y. and Weyers, R. E., "Modeling the Time-to-Corrosion Cracking in Chloride Contaminated Reinforced Concrete Structures," Corrosion, 1998, Vol.95, pp. 675-681.
5. Chernin, L., Val, D. V. and Volokh, K. Y., "Analytical modelling of concrete cover cracking caused by corrosion of reinforcement," Materials and Structures, 2010, Vol.43, pp. 543-556.
6. Molina, F., Alonso, C. and Andrade, C., "Cover cracking as a function of rebar corrosion: Part 2—Numerical model," Materials and Structures, 1993, Vol.26, pp. 532-548.
7. Noghabai, K., "FE-Modelling of cover splitting due to corrosion by use of inner softening band," Materials and Structures, 1999, Vol.32, pp. 486-491.
8. Biondini, F. and Vergani, M., "Damage modeling and nonlinear analysis of concrete bridges under corrosion,". roc. of 6th International Conference on Bridge Maintenance, Safety and Management, July, 2012, pp. 949-957.
9. Isgor, O. B. and Razaqpur, A. G.,"Modelling steel corrosion in concrete structures," Materials and Structures, 2006, Vol.39, pp. 291-302.
10. Michel, A., Solgaard, A.O.S., Geiker, M., Stang, H. and Olesen, J.F., "Modeling Formation of Cracks in Concrete Cover due to Reinforcement Corrosion," Proc. of 7th International Conference on Fracture Mechanics of Concrete & Concrete Structures, May, 2010, pp.944-951.
11. Solgaard, A. O. S., Michel, A., Geiker, M., and Stang, H., "Concrete Cover Cracking due to Uniform Reinforcement Corrosion," Materials and Structures, 2013.
12. Michel, A., Pease, B.J., Peterová, A. and Geiker, M., "Experimental determination of the penetration depth of corrosion products and time to corrosion-induced cracking in reinforced cement based materials," Proc. of International. Congress On Durability of Concrete, July, 2012.
13. Pease, B. J., Michel, A. and Stang, H., "Quantifying movements of corrosion products in reinforced concrete using x-ray attenuation measurements" Proc. of the 2nd International Conference on Microstructure Related Durability of Cementitious Composites, 2012.
14. Michel, A., Pease, B. J., Geiker, M., Stang, H. and Olesen, J. F., "Monitoring reinforcement corrosion

and corrosion-induced cracking using non-destructive x-ray attenuation measurements," Cement and Concrete Research, 2011, Vol.41, pp. 1085-1094.
15. Pease, B. J., Michel, A., Thybo, A. E. A. and Stang, H., "Estimation of elastic modulus of reinforcement corrosion products using inverse analysis of digital image correlation measurements for input in corrosion-induced cracking model," Proc. of 6th International Conference on Bridge Maintenance, Safety and Management, July, 2012, pp.3643-3650.
16. Thybo, A. E. A., Michel, A. and Stang, H., "Modeling of Corrosion-induced Concrete Damage," VIII International Conference on Fracture Mechanics of Concrete and Concrete Structures, 2013, Submitted.
17. Tuutti, K., "Corrosion of steel in concrete," Swedish Cement and Concrete Research Institute, 1982, Report 4‐82.
18. fib, "Model code for service life design," International Federation for Structural Concrete, 2006, Tech. Rep. fib Bulletin 34.
19. European Committee for Standardization, "Eurocode 2: Design of concrete structures - Part 1-1: General rules and rules for buildings," Danish Standard, 2008, pp. 29-30.
20. Aalborg Portland, "Cement og beton," Aalborg Portland A/S, 2013, pp.89.